

The Cellular Basis for Enhanced Volume-modulated Cardiac Output in Fish Hearts

Holly A. Shiels,^{1,2} Sarah C. Calaghan,¹ and Ed White¹

¹Institute of Membrane and Systems Biology, University of Leeds, Leeds, LS2 9JT, UK

²Faculty of Life Sciences, 2.18c Core Technology Facility, University of Manchester, Manchester, M13 9NT, UK

During vertebrate evolution there has been a shift in the way in which the heart varies cardiac output (the product of heart rate and stroke volume). While mammals, birds, and amphibians increase cardiac output through large increases in heart rate and only modest increases (~30%) in stroke volume, fish and some reptiles use modest increases in heart rate and very large increases in stroke volume (up to 300%). The cellular mechanisms underlying these fundamentally different approaches to cardiac output modulation are unknown. We hypothesized that the divergence between volume modulation and frequency modulation lies in the response of different vertebrate myocardium to stretch. We tested this by progressively stretching individual cardiac myocytes from the fish heart while measuring sarcomere length (SL), developed tension, and intracellular Ca^{2+} ($[\text{Ca}^{2+}]_i$) transients. We show that in fish cardiac myocytes, active tension increases at SLs greater than those previously demonstrated for intact mammalian myocytes, representing a twofold increase in the functional ascending limb of the length–tension relationship. The mechanism of action is a length-dependent increase in myofilament Ca^{2+} sensitivity, rather than changes in the $[\text{Ca}^{2+}]_i$ transient or actin filament length in the fish cell. The capacity for greater sarcomere extension in fish myocardium may be linked to the low resting tension that is developed during stretch. These adaptations allow the fish heart to volume modulate and thus underpin the fundamental difference between the way fish and higher vertebrates vary cardiac output.

INTRODUCTION

All vertebrate cardiac muscle responds intrinsically to stretch by increasing contractile strength, the Frank-Starling law of the heart. Consequently, an increase in end-diastolic ventricular volume increases stroke volume via a stretch-induced increase in myocardial contractility (Allen and Kentish, 1985). However, the relative importance of the Frank-Starling mechanism for increasing cardiac output (the product of heart rate and stroke volume) varies immensely among vertebrates. The fish heart can dramatically increase cardiac output by modulating stroke volume, relying less on increasing heart rate. Fish hearts can therefore be distinguished from mammalian hearts by being capable of considerably larger changes in stroke volume (Farrell and Jones, 1992; Burggren et al., 1997). Indeed, stroke volume can triple in some fish species with only small increases (0.2–0.3 kPa) in filling pressure (Farrell and Olson, 2000). In contrast, birds and mammals rely on frequency modulation to a far greater extent than volume modulation to vary cardiac output, e.g., pigeon heart rate can increase more than sixfold between rest and flight with no change in stroke volume (Peters et al., 2005). Frequency modulation and volume modulation are both effective strategies

for regulating cardiac output to meet changing cardiovascular demands. However, differences in cardiac design are expected between hearts that operate at the extremes of each strategy. There are numerous studies on the cellular factors that have permitted the generation of fast heart rates during vertebrate evolution (for review see Lillywhite et al., 1999). However, no studies have addressed the cellular adaptations that allow the myocardium of lower vertebrates to predominantly volume modulate.

We report the first cellular investigation of the Frank-Starling mechanism in fish cardiac myocytes. We used carbon fiber transducers to investigate stretch-induced increases in sarcomere length (SL), developed tension, and intracellular Ca^{2+} ($[\text{Ca}^{2+}]_i$) transients in single trout (*Oncorhynchus mykiss*) ventricular myocytes in order to describe the SL–tension relationship. Our results show that the functional ascending limb of the length–tension relationship is extended twofold in trout compared with mammals. Differences in myofilament overlap cannot account for this, as we show thin filament length in trout is not different from that in rat. This extended functional length–tension relationship is achieved without changes in the amplitude of the $[\text{Ca}^{2+}]_i$ transient, indicating a stretch-induced

Correspondence to Holly Shiels: holly.shiels@manchester.ac.uk

The online version of this article contains supplemental material.

Abbreviation used in this paper: SL, sarcomere length.

increase in the sensitivity of the myofilaments to Ca^{2+} . This cellular adaptation is critical for allowing the sarcomeres of fish myocytes to develop tension while accommodating the large blood volume changes necessary for volume modulating cardiac output.

MATERIALS AND METHODS

Animals

Female rainbow trout (*Oncorhynchus mykiss*, mean body mass of 137 ± 5 g, $n = 83$) were purchased from Glasshouses Trout farm (Glasshouses, North Yorkshire, UK). They were held indoors in large fiberglass tanks containing recirculated aerated fresh water for a minimum of 2 wk at 15°C before experimentation. Male Wistar rats were maintained in cages of four animals. Both species were exposed to a 12 h:12 h, light:dark photoperiod and fed ad libitum with appropriate commercial pellets. All animal procedures are in accordance with UK regulations. Myocytes were isolated via enzymatic digestion in a modified Langendorf preparation. A detailed description of the myocyte preparation has been published previously for both rainbow trout (Vornanen, 1998; Shiels et al., 2000) and rat (Calaghan et al., 1998).

Measurement of Auxotonic Contractions and Axial Stretch

Fish myocytes were placed on the stage of an inverted microscope (Nikon, Eclipse) and superfused with a physiological saline of the following composition (in mM): NaCl, 150; KCl, 5.4; MgSO_4 , 1.2; NaH_2PO_4 , 0.4; CaCl_2 , 2.0; glucose, 5; pyruvate 5; HEPES, 10. KOH was used to adjust pH to 7.8, which is the pH of interstitial fluid in fresh water teleosts. Unlike mammalian myocytes, fish ventricular myocytes are long ($>100 \mu\text{m}$) and thin; mean cell width was $7.55 \pm 0.85 \mu\text{m}$, $n = 31$ cells.

Carbon fiber transducers were attached toward either end of the myocyte $\sim 100 \mu\text{m}$ apart, in order to record tension and to stretch myocytes along their longitudinal axis (Le Guennec et al., 1990; Calaghan and White, 2004). A single flexible carbon fiber (diameter $12 \mu\text{m}$, length 2 mm, compliance 80 m N^{-1}) was attached toward one end and a stiffer double fiber (length 0.8 mm, compliance 0.3 m N^{-1}) was attached toward the other. Fibers were mounted in the ends of microelectrodes that were attached to micromanipulators. The displacement of the single fiber during contractions was used to calculate the force developed. Myocytes were field stimulated to contract, using platinum electrodes delivering suprathreshold pulses of 10 ms duration, at 0.5 Hz. The cell was stretched by movement of the stiff fiber. SL–tension relationships were measured by progressively stretching the cells by small increments, with ~ 12 contractions between stretches. An image of the cell from a CCD camera enabled the position of fibers to be continuously monitored via a video edge detection system (Crescent Electronics). Please see the online supplemental material (Video 1, available at <http://www.jgp.org/cgi/content/full/jgp.200609543/DC1>) for a video of an experiment. Because the cells develop force and shorten, they contract auxotonically, as occurs during the systolic ejection phase. Passive force was measured as end diastolic force assuming zero passive force at slack length. Active force was the additional force developed during systole. Total force was the sum of these two. Force was normalized to the cross-sectional area of each myocyte, assuming an elliptical cross section. Stretch was indexed as the increased end diastolic SL between the fibers measured from the video image of the cell, projected onto a large screen. SL measurements were calibrated with a graticule slide. SL–tension relationships are plotted using end diastolic SL. It is acknowledged that SL shortening will occur during systole, in a manner dependent upon the degree of cell shortening.

Assessment of Actin Filament Length

Aliquots of ventricular myocytes isolated from trout or male Wistar rats were suspended in physiological HEPES-based buffer and plated on poly-lysine-coated slides. After adherence, cells were resuspended in HEPES-based buffer containing 0, 2, or 5 mM added Ca^{2+} for 1 min, and then fixed for 30 min with 4% paraformaldehyde containing the same concentration of Ca^{2+} . Myocytes were permeabilized for 20 min with 0.1% Triton X-100 in PBS, blocked with PBS containing 1% BSA and 10% donkey serum for 1 h, and incubated with PBS containing $0.1 \mu\text{M}$ rhodamine-phalloidin and 1% BSA for 20 min. Optical sections of $\sim 2 \mu\text{m}$ thickness were acquired by confocal laser microscopy (Carl Zeiss MicroImaging, Inc. LSM 5 Pascal). On-line fast Fourier transformation of striated patterning was performed in each myocyte (LSM software; see Fig. 4 A for details of this methodology). Myocytes were assigned, on the basis of visual inspection, supported by fast Fourier transform analysis, to one of three categories: bare patch evident in center of sarcomere, actin overlap evident in center of sarcomere, and neither bare patch nor overlap evident in the sarcomere. The mean SL (distance from Z-line to Z-line) of cells in the latter category was used to estimate actin filament length in the two species (see Fig. 4).

Measurement of Fura-2 Fluorescence

To record changes in $[\text{Ca}^{2+}]_i$, some cells were loaded with the fluorescent Ca^{2+} indicator Fura-2 AM for 6 min at $3 \mu\text{M}$ final concentration. The ratio of the fluorescence emitted by cells at 510 nm in response to alternate illumination with light at 340 and 380 nm (Cairn Research) was used as our index of $[\text{Ca}^{2+}]_i$ (Calaghan and White, 2004).

Online Supplemental Material

See the supplemental material (Video 1, available at <http://www.jgp.org/cgi/content/full/jgp.200609543/DC1>) for a video recording of a single trout ventricular myocyte attached to carbon fibers and stretched from slack SL of $1.83 \mu\text{m}$ to SL of $2.5 \mu\text{m}$. This recording is for the same cell that appears as still images in Fig. 1 A. The cell was stimulated to contract at 0.5 Hz. Note the stretching of the myocyte by the righthand fiber. The lefthand fiber is $12 \mu\text{m}$ in diameter, and it bends, during contraction, as the cell is progressively stretched. The black bars with white central dots come from the edge detection equipment used to monitor fiber position. The video is not a continuous record, some excitations between stretches have been edited out, and the play speed is two times normal speed to shorten the length of the video.

RESULTS

The mean end diastolic SL of stimulated trout myocytes was $1.84 \pm 0.02 \mu\text{m}$ at slack length ($n = 31$ myocytes from 13 hearts). This is similar to diastolic SLs for electrically stimulated rat myocytes. To demonstrate responsiveness to Ca^{2+} , stimulation was stopped and cells were superfused with solution containing no added Ca^{2+} . Under these conditions, trout SL increased from $1.84 \pm 0.03 \mu\text{m}$ to $1.93 \pm 0.04 \mu\text{m}$ ($P < 0.05$, paired Student's *t* test, $n = 12$ cells).

When trout myocytes were electrically stimulated to contract and incrementally stretched (Fig. 1 A and Video 1), there was a progressive increase in both passive tension and active tension (Fig. 1 B). It was immediately apparent that fish myocytes could be stretched more than the mammalian myocytes typically studied in

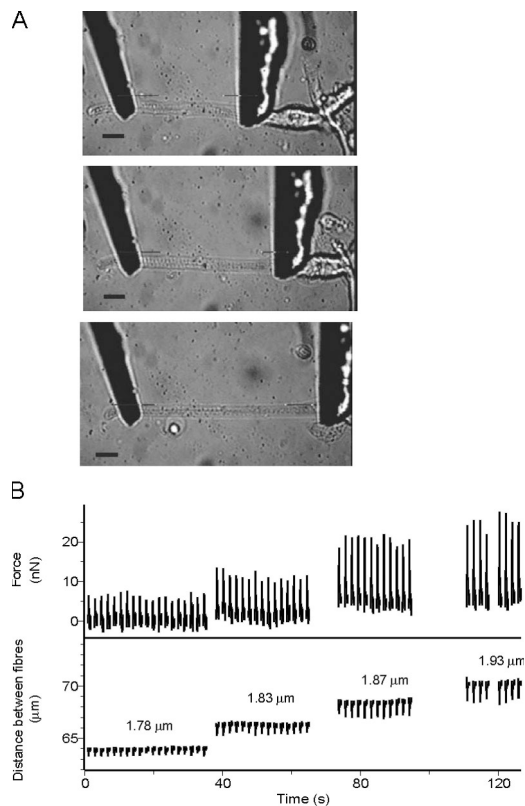


Figure 1. Stretch of single trout ventricular myocytes. (A) Single trout ventricular myocyte held between two carbon fibers. Images show the myocyte at slack length (top, SL $1.80\ \mu\text{m}$), and following stretches to SL $2.16\ \mu\text{m}$ (middle) and $2.50\ \mu\text{m}$ (bottom). An on-line video of this experiment is available (Video 1). Bar, $10\ \mu\text{m}$. (B) Data from a different cell showing how progressive stretching increases passive and active tension (top trace), when the distance between the fibers is increased, causing stretch of the sarcomere (bottom trace, numbers show diastolic SL at each stretch).

our laboratory (i.e., from ferret, rat, or guinea pig, White et al., 1995; Cazorla et al., 2000a). Fig. 2 shows SL–tension relations for passive and total tension from two individual trout myocytes (Fig. 2, A and B) and mean data (Fig. 2 C). The SL–passive tension relationship in trout myocytes remained essentially linear even with extensions up to 40%.

Fig. 3 (A and B) shows examples of the large increases in active tension with stretch in individual trout myocytes. Fig. 3 (C and D) shows the corresponding ascending limbs and in Fig. 3 D a peak and the beginning of a descending limb of the length–tension relationship. The mean length–active tension relationship for rainbow trout myocytes are plotted against data for rat and ferret ventricular myocytes (taken from Cazorla et al., 2000a) derived using the same carbon fiber technique (Fig. 3 E). The comparison is made only for the range of SLs where the data from trout and the mammalian species overlap. There is no difference in the steepness of the SL–active tension relationship or in force, corrected for cross-sectional area, over this range of SLs. In intact mammalian

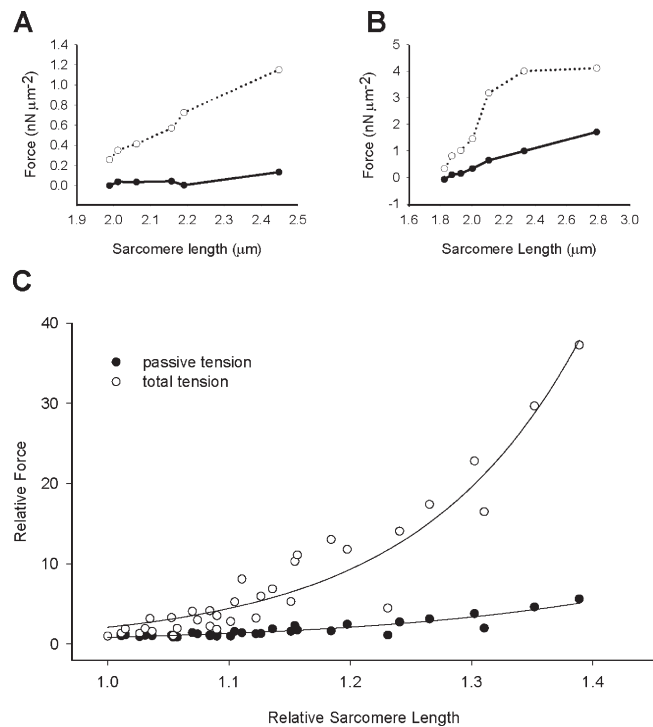


Figure 2. Effect of stretch on passive tension and total tension in single trout ventricular myocytes. (A and B) SL–tension relationships showing both passive tension (filled circles) and total tension (open circles) for two individual trout myocytes. (C) Mean SL–tension relationships ($n = 9$ myocytes from five fish) normalized to relative scales where $1.0 = 1.84 \pm 0.04\ \mu\text{m}$ for x axis and $1.0 = 0.20 \pm 0.04\ \text{nN}\ \mu\text{m}^{-2}$ for y axis. Passive tension at slack length (i.e., where $1.0 = 1.84 \pm 0.04$) is set to zero.

myocardium, L_{max} (length at peak active tension) is reached at a diastolic SL of $\sim 2.2\text{--}2.3\ \mu\text{m}$, after a 20–25% stretch from slack length ($\sim 1.83\ \mu\text{m}$) (Allen and Kentish, 1985, and see Discussion). In contrast, Fig. 3 F shows that active force in fish myocytes increases when SL is increased by 40%, suggesting L_{max} occurs at or above a diastolic SL of $2.6\ \mu\text{m}$.

Our observation of an extended functional length–tension relationship may explain how fish are able to modulate cardiac output with large changes in blood volume. But how is this extended ascending limb achieved? One explanation is differences in sarcomere anatomy between vertebrate classes as the diastolic SL at L_{max} is related to the degree of thick (myosin) and thin (actin) filament overlap, which in turn will depend on thick and thin filament length. Little variation in myosin filament length is found in relaxed vertebrate muscle, but actin filament length is species and muscle type dependent (Robinson and Winegrad, 1979; Granzier et al., 1991). Thus we hypothesized that the actin filaments were longer in fish than mammals, which would facilitate maximum cross-bridge availability at longer sarcomere lengths and extend the ascending limb of the length–tension

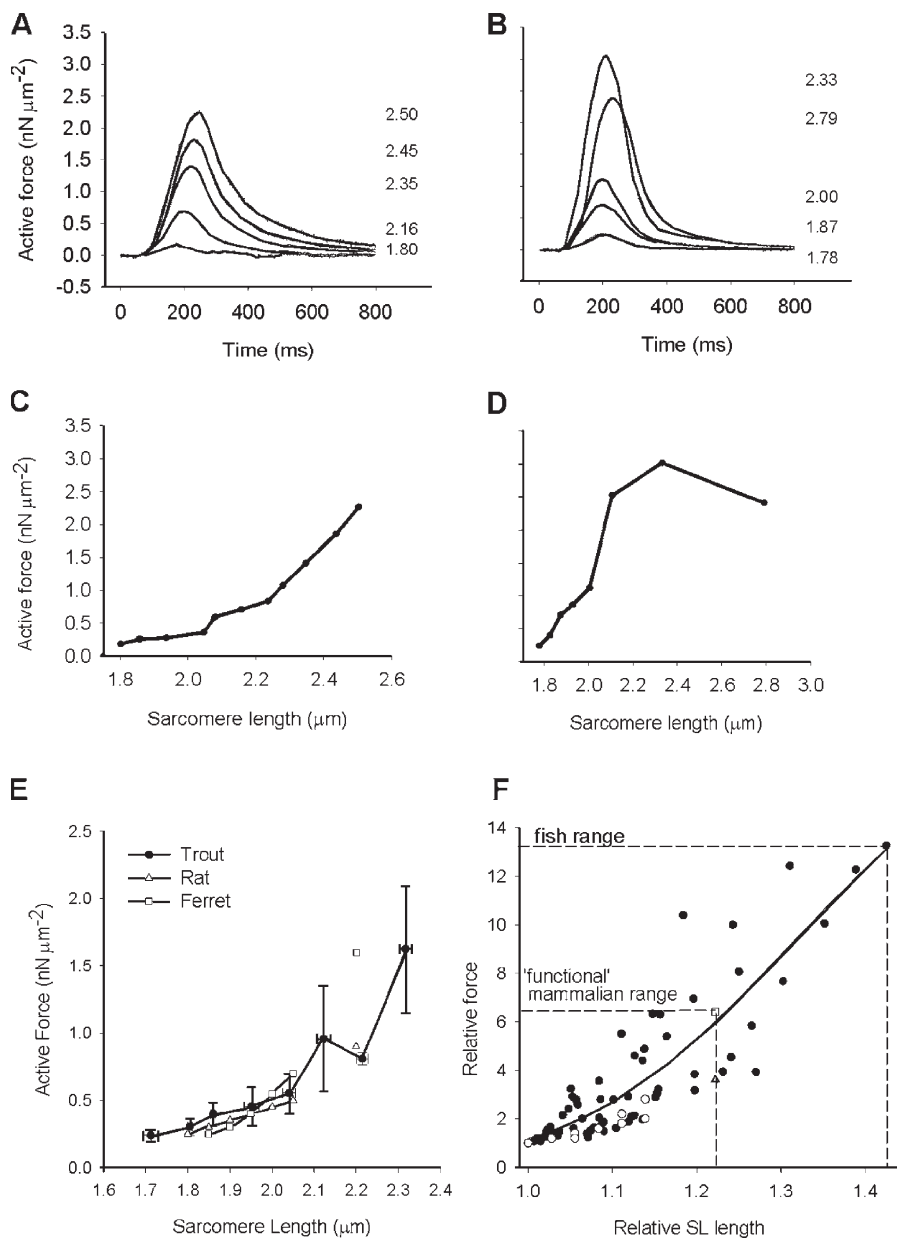


Figure 3. Effect of stretch on active tension in single trout ventricular myocytes. (A and B) Stretch-induced increase in active tension in two myocytes at selected diastolic SL (shown to the right). (C and D) SL-active tension relationships in the same cells. (E) Mean diastolic SL-active tension relationship for rainbow trout ($n = 9$ myocytes from five fish) that provided several data points for SLs below $2.2\text{--}2.3\ \mu\text{m}$ in order to compare with data for rat (open triangle) and ferret (open squares) ventricular myocytes, replotted from Cazorla et al. (2000a). The unconnected open square (ferret) and open triangle (rat) extrapolates the mammalian length-tension relationships to $2.2\ \mu\text{m}$. (F) Mean SL-active tension relationships (31 myocytes from 13 fish; closed circles) normalized to relative scales, where $1.0 = 1.84 \pm 0.02\ \mu\text{m}$ for x axis and $1.0 = 0.19 \pm 0.03\ \text{nN}\ \mu\text{m}^{-2}$ for y axis. Mammalian data as in E.

relationship. To test this hypothesis, we compared the length of the actin filament in trout and rat ventricular myocytes (Fig. 4). By increasing added Ca^{2+} in the solution from 0 to 5 mM we were able to visualize shortening of the sarcomere and estimate the length of the actin filament (see Materials and Methods). Trout myocytes in 0 mM added Ca^{2+} had a sarcomeric spacing of $2.03 \pm 0.04\ \mu\text{m}$ ($n = 3$) and showed a distinct area of low fluorescence within individual sarcomeres (Fig. 4 A, right). We interpret this region as the thick (myosin) filament in the absence of overlapping thin (actin) filament (H band). As added Ca^{2+} was increased, sarcomeric spacing fell, and the area of low fluorescence disappeared at a spacing of $1.90 \pm 0.02\ \mu\text{m}$ ($n = 8$, Fig. 4 A, center),

to be replaced by a band of high fluorescence, prominent at a sarcomeric spacing of $1.62 \pm 0.03\ \mu\text{m}$ ($n = 20$, Fig. 4 A, left). We interpret the band of high fluorescence intensity as double overlapping of the actin filaments from opposite ends of the sarcomere. As neither H band nor overlap were detected at a mean SL of $1.90\ \mu\text{m}$ we conclude that in trout myocytes the length of the thin actin myofibril is close to $0.95\ \mu\text{m}$ (Fig. 4 C). This value is similar to previous measurements of thin filament length in vertebrate striated muscle (Page, 1964; Burkholder and Lieber, 2001) and, importantly for the present interpretation, is not different to that which we measured in rat myocytes undergoing the same treatment (Fig. 4, B and C). Therefore, thin filament length cannot explain the

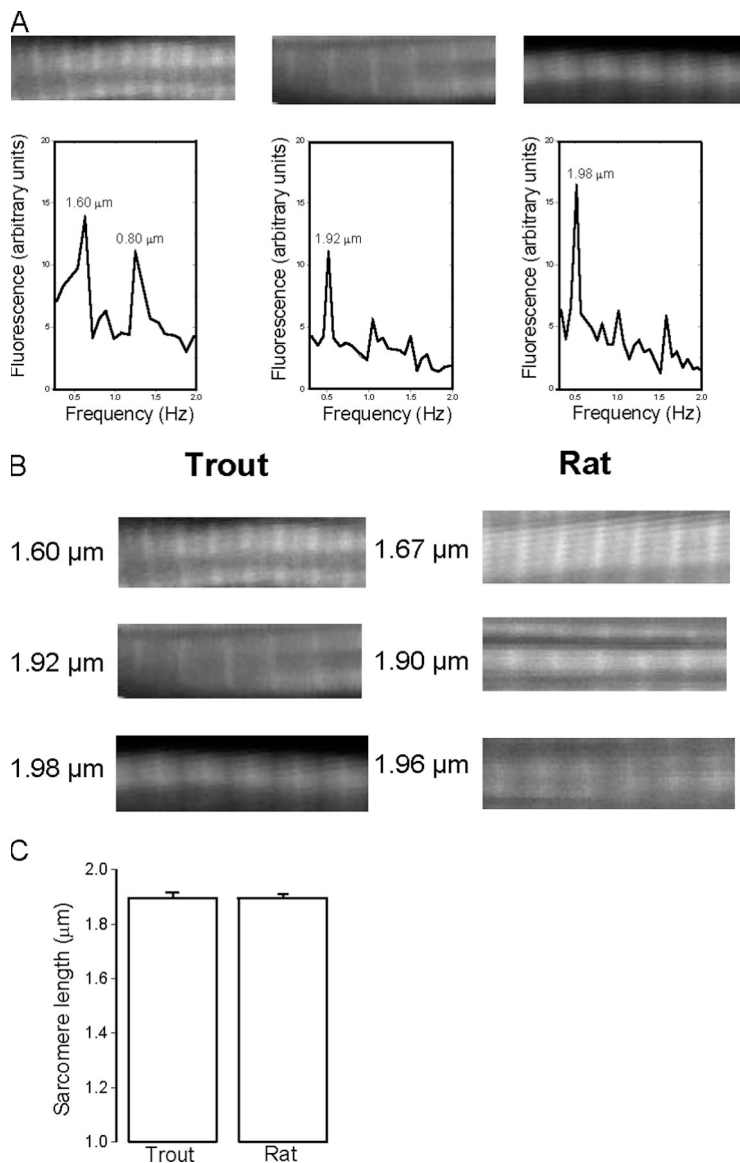


Figure 4. Relationship between actin banding pattern and SL in ventricular myocytes from trout and rat. (A) Confocal images (above) and associated fast Fourier transformations (below) representative of the three categories of sarcomeric banding patterns in trout ventricular myocytes. Left (5 mM Ca^{2+}), a myocyte with SL of 1.60 μm showing actin overlap in the center of the sarcomere, giving rise to two peaks on the fast Fourier transformation. Center (2 mM Ca^{2+}), a myocyte with an SL of 1.92 μm shows neither overlap nor a bare patch. The only peak on the fast Fourier transformation corresponds to the SL. Right (0 mM Ca^{2+}), a myocyte with a SL of 1.98 μm shows evidence of a bare patch in the center of the sarcomere. (B) Confocal microscopy images of myocytes from trout (left) and rat (right) representative of the three categories of sarcomeric banding showing actin overlap between bright Z-lines (top), neither overlap nor bare patch (middle), and a bare patch in the center of the sarcomere (bottom). (C) The mean sarcomere length for trout ($n = 8$) and rat ($n = 12$) myocytes showing neither bare patch nor overlap was identical at 1.90 μm ($P > 0.05$). Therefore actin filament length in both species is $\sim 0.95 \mu\text{m}$.

extended ascending length–tension relationship in the fish myocardium.

Actin and myosin overlap does not, however, strictly dictate the shape of the length–tension relationship. Increased myofilament Ca^{2+} sensitivity could explain our observed increase in active force generation past optimum myofilament overlap in the fish sarcomere. We tested this hypothesis in trout myocytes by simultaneously monitoring changes in force and $[\text{Ca}^{2+}]_i$ in response to stretch. We found a progressive increase in force with each stretch, in the absence of an increase in the amplitude of the $[\text{Ca}^{2+}]_i$ transient (Fig. 5). This finding is in line with previous studies in mammalian cardiac tissue and single myocytes (Allen and Kurihara, 1982; Allen and Kentish, 1985; White et al., 1993, 1995; Hongo et al., 1996; Calaghan and White, 2004). Thus, we conclude that the major mechanism associated with the stretch-induced increase in force in trout myocytes

is a stretch-induced increase in myofilament Ca^{2+} sensitivity, defined here as an increase in force for a given level of $[\text{Ca}^{2+}]_i$.

DISCUSSION

In intact mammalian cardiac trabeculae it has been shown that the length at which maximum active tension occurs (L_{max}) corresponds to an SL of 2.2–2.3 μm ; stretch beyond this point leads to a fall in active tension with no increase in the SL of the sarcomeres in the center of the preparation (e.g., ter Keurs et al., 1980; Allen and Kentish, 1985; Kentish et al., 1986). Likewise, in single cardiac myocyte studies, our attempts to stretch mammalian cells beyond an SL of 2.2–2.3 μm have been largely unsuccessful. Thus, the functional peak of the ascending limb of the SL–active tension relationship in intact mammalian myocardium occurs at an SL of 2.2–2.3 μm , even

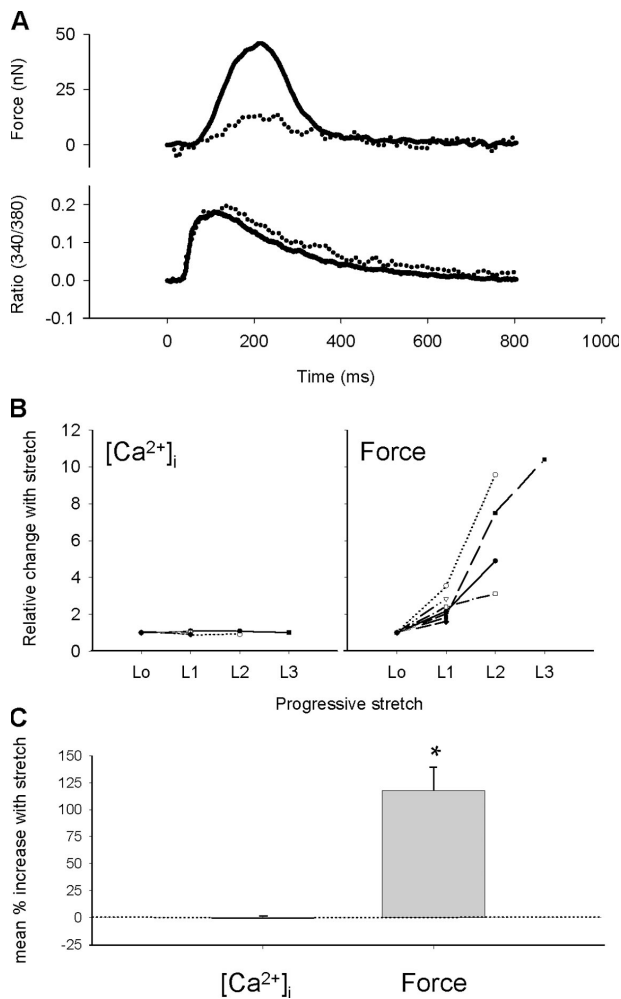


Figure 5. Stretch increases active tension but not the amplitude of the $[Ca^{2+}]_i$ transient. (A) Simultaneous measurement of changes in tension (top) and intracellular Ca^{2+} ($[Ca^{2+}]_i$) measured with fura-2 (bottom) at slack length (dotted line) and after a stretch (solid line). (B) Progressive stretching from a slack length SL of $\sim 1.84 \mu\text{m}$ at Lo to length 1 (L1, $\sim 2.0 \mu\text{m}$), length 2 (L2, $\sim 2.3 \mu\text{m}$), and length 3 (L3, $\sim 2.39 \mu\text{m}$) did not increase the amplitude of the $[Ca^{2+}]_i$ transient (left) but did increase active tension ($n = 7$ cells, individual lines). (C) Mean percent increase in the $[Ca^{2+}]_i$ and in force with stretch (to maximum length for each cell), $n = 7$. * indicates significant increase in force with stretch $P < 0.00001$, Mann-Whitney test.

though work in skinned myocytes suggests a longer peak SL may exist for the myofilaments in isolation (Fabiato and Fabiato, 1978).

By conducting the first study of the SL–tension relationship of fish cardiac myocytes, we have demonstrated an extended functional ascending limb of the SL–tension relationship. Comparing these results with data from mammalian myocytes shows that this critical cellular adaptation allows fish myocytes to be stretched by 40%, twice as much as their mammalian counterparts, and still increase active force. In trout myocytes, myocardial force increases >12 -fold between slack

length and maximum SL (Fig. 3). In mammalian myocytes (Cazorla et al., 2000a) and mammalian trabeculae (Kentish et al., 1986), the increase in force with stretch between slack and the maximum SLs recorded is closer to fivefold. The slopes of the SL–active tension relationship for fish and mammals (at least at SLs that can be compared, see Fig. 3, E and F) appears similar, and, in common with mammalian species, there is no immediate increase in the amplitude of the trout $[Ca^{2+}]_i$ transient upon stretch. Thus the species difference arises from an extended ascending limb rather than a steeper ascending limb. An important consequence of this difference in cardiac design is that the fish heart will maintain myocardial pressure when stretched by large blood volumes whereas the mammalian heart will not. The large (>10 -fold) increases in force associated with 40% stretches in trout myocytes (Fig. 3 F) is probably vital for maintaining pressure development in the distended fish myocardium in accordance with Laplace’s law.

The trout has a pyramid-shaped ventricle, with similar length and height (Franklin and Davie, 1992). To accommodate a threefold increase in stroke volume, as can occur with exercise (Farrell and Jones, 1992), an extension of $\sim 40\%$ along the major axes is required. Therefore, our finding of a 40% increase in SL from slack length directly relates to known physiologically relevant myocardial stretch of the whole heart.

Our finding of similar actin filament length in fish and rat cardiac myocytes of $\sim 0.95 \mu\text{m}$ indicates that tension generation in the fish sarcomere continues to increase beyond optimum overlap of actin and myosin filaments. The exquisite extensibility of the isolated single fish myocyte (Fig. 1 A, and Video 1) is likely to be associated with their much smaller cross-sectional area and the lower levels of passive tension per unit area in fish compared with mammalian myocytes. Trout myocyte passive tension ($1.3 \text{ nN } \mu\text{m}^{-2}$ over a comparable range of SLs, $1.8\text{--}2.1 \mu\text{m}$) was less than that previously measured in mammalian myocytes ($\sim 2\text{--}4 \text{ nN } \mu\text{m}^{-2}$ per μm increase in SL, depending on species, Cazorla et al., 1997, 2000a). However it is interesting that the passive tension curve of trout myocytes remains relatively shallow and essentially linear compared with active tension with SL extension up to 40%, while in both intact mammalian tissue (e.g., Kentish et al., 1986) and skinned single myocytes (e.g., Cazorla et al., 2000b; Wu et al., 2000; but see Fabiato and Fabiato, 1978), large, exponential increases of passive tension are typical for stretches of 20%. Species differences in the length of collagen fibers (Hanley et al., 1999) may be important in explaining these differences at the level of the tissue or the whole heart. As discussed further below, variable isoforms of the giant myofilament protein titin may also be involved in cellular differences in passive tension between species.

It is important to point out that the steepness of the active SL–tension curve will be affected by the degree of Ca^{2+} activation (see Fabiato and Fabiato, 1978). By using intact cardiac myocytes, we were unable to control the degree of Ca^{2+} activation as cytosolic Ca^{2+} was free to change in a physiological way in response to the action potential. Future studies could use skinned preparations to address this issue specifically.

The positive inotropic effect of adrenergic stimulation in mammalian hearts can increase stroke volume independently of the Frank-Starling mechanism by increasing ejection fraction. Although adrenergic stimulation increases inotropy in fish hearts, there is less scope for an increase in ejection fraction, which is very high even under resting conditions (Farrell and Jones, 1992). In fish, adrenergic-induced inotropy would therefore appear to assist the Frank-Starling mechanism by pumping larger end diastolic volumes.

Stretch may result in the formation of more optimal geometry for interaction between actin and myosin, a factor important in the stretch-induced increase in Ca^{2+} sensitivity (Godt and Maughan, 1981, but see Konhilas et al., 2002). The elasticity of cardiac muscle and the compression of the myofilament lattice spacing, at SLs on the ascending limb, are largely determined by titin (Granzier and Irving, 1995; Fukuda et al., 2003), with variations between mammalian species being determined by the levels of isoforms expressed (Cazorla et al., 2000b). We attempted to assess the isoform(s) of fish titin using SDS-PAGE techniques that we have successfully used to identify titin isoforms in mammalian cardiac tissue (see Natali et al., 2002). However, we were not successful due to the lack of antibody specificity with the fish muscle. Thus at present, the titin isomer(s) of fish myocardium remain unknown. Earlier work comparing the Ca^{2+} sensitivity of tension in skinned fibers from fish and mammals has shown that the fish myocardium has a greater inherent Ca^{2+} sensitivity (Churcott et al., 1994), partially due to the greater affinity of fish troponin C for Ca^{2+} (Gillis et al., 2000). The length-dependent changes in myofilament Ca^{2+} sensitivity in fish and mammals has yet to be compared.

In trout, the Frank-Starling mechanism is an effective and powerful strategy for regulating cardiac output. Indeed, although there are a few notable exceptions (Farrell, 1996; Rantin et al., 1998), the maximum heart rate of most fish species does not exceed 2 Hz (~120 bpm), irrespective of temperature or level of adrenergic stimulation (Farrell, 1991). Their capacity to vary cardiac output by increasing heart rate is therefore limited. In contrast, higher vertebrates can modulate cardiac output via large changes in cardiac frequency, thus a shorter ascending SL–tension relationship, which limits volume modulation, does not limit myocardial function.

Carbon fibers were a gift from Prof. Jean-Yves LeGuenec (Université de Tours, Tours, France).

This work was supported by a Natural Sciences and Engineering Research Council of Canada post-doctoral fellowship to H.A. Shiels, the University of Leeds, and the University of Manchester.

Olaf S. Andersen served as editor.

Submitted: 22 March 2006

Accepted: 26 May 2006

REFERENCES

- Allen, D.G., and S. Kurihara. 1982. The effects of muscle length on intracellular calcium transients in mammalian cardiac muscle. *J. Physiol.* 327:79–94.
- Allen, D.G., and J. Kentish. 1985. The cellular basis of the length-tension relation in cardiac muscle. *J. Mol. Cell. Cardiol.* 17:821–840.
- Burggren, W., A.P. Farrell, and H. Lillywhite. 1997. Vertebrate cardiovascular systems. In *The Handbook of Physiology*. W.H. Dantzer, editor. Oxford University Press, New York. 215–308.
- Burkholder, T.J., and R.L. Lieber. 2001. Sarcomere length operating range of vertebrate muscles during movement. *J. Exp. Biol.* 204:1529–1536.
- Calaghan, S.C., and E. White. 2004. Activation of Na^+ - H^+ exchange and stretch-activated channels underlies the slow inotropic response to stretch in myocytes and muscle from the rat heart. *J. Physiol.* 559:205–214.
- Calaghan, S.C., E. White, and J. Colyer. 1998. Co-ordinated changes in cAMP, phosphorylated phospholamban, Ca^{2+} and contraction following beta-adrenergic stimulation of rat heart. *Pflugers Arch.* 436:948–956.
- Cazorla, O., C. Pascarel, D. Garnier, and J.Y. Le Guennec. 1997. Resting tension participates in the modulation of active tension in isolated guinea pig ventricular myocytes. *J. Mol. Cell. Cardiol.* 29:1629–1637.
- Cazorla, O., J.Y. Le Guennec, and E. White. 2000a. Length-tension relationships of sub-epicardial and sub-endocardial single ventricular myocytes from rat and ferret hearts. *J. Mol. Cell. Cardiol.* 32:735–744.
- Cazorla, O., A. Freiburg, M. Helmes, T. Centner, M. McNabb, Y. Wu, K. Trombitas, S. Labeit, and H. Granzier. 2000b. Differential expression of cardiac titin isoforms and modulation of cellular stiffness. *Circ. Res.* 86:59–67.
- Churcott, C.S., C.D. Moyes, B.H. Bressler, K.M. Baldwin, and G.F. Tibbits. 1994. Temperature and pH effects on Ca^{2+} sensitivity of cardiac myofibrils: a comparison of trout with mammals. *Am. J. Physiol.* 267:R62–R70.
- Fabiato, A., and F. Fabiato. 1978. Myofilament-generated tension oscillations during partial calcium activation and activation dependence of the sarcomere length-tension relation of skinned cardiac cells. *J. Gen. Physiol.* 72:667–699.
- Farrell, A.P. 1991. From hagfish to tuna: a perspective on cardiac function in fish. *Physiol. Biochem. Zool.* 64:1137–1164.
- Farrell, A.P. 1996. Features heightening cardiovascular performance in fishes; with special reference to tunas. *Comp. Biochem. Physiol. A.* 113:61–67.
- Farrell, A.P., and D.R. Jones. 1992. The Heart. In *The Cardiovascular System*. W.S. Hoar, D.J. Randall, and A.P. Farrell, editors. Academic Press, San Diego, CA. 1–88.
- Farrell, A.P., and K.R. Olson. 2000. Cardiac natriuretic peptides: a physiological lineage of cardioprotective hormones? *Physiol. Biochem. Zool.* 73:1–11.
- Franklin, C.E., and P.S. Davie. 1992. Dimensional analysis of the ventricle of an in situ perfused trout heart using echocardiography. *J. Exp. Biol.* 166:47–60.

- Fukuda, N., Y. Wu, G. Farman, T.C. Irving, and H. Granzier. 2003. Titin isoform variance and length dependence of activation in skinned bovine cardiac muscle. *J. Physiol.* 553:147–154.
- Gillis, T.E., C.R. Marshall, X.H. Xue, T.J. Borgford, and G.F. Tibbits. 2000. Ca²⁺ binding to cardiac troponin C: effects of temperature and pH on mammalian and salmonid isoforms. *Am. J. Physiol. Regul. Integr. Comp. Physiol.* 279:R1707–R1715.
- Godt, R.E., and D.W. Maughan. 1981. Influence of osmotic compression on calcium activation and tension in skinned muscle fibers of the rabbit. *Pflügers Arch.* 391:334–337.
- Granzier, H.L., H.A. Akster, and H.E. ter Keurs. 1991. Effect of thin filament length on the force-sarcomere length relation of skeletal muscle. *Am. J. Physiol.* 260:C1060–C1070.
- Granzier, H.L., and T.C. Irving. 1995. Passive tension in cardiac muscle—contribution of collagen, titin, microtubules, and intermediate filaments. *Biophys. J.* 68:1027–1044.
- Hanley, P.J., A.A. Young, I.J. LeGrice, S.G. Edgar, and D.S. Loiselle. 1999. 3-Dimensional configuration of perimysial collagen fibres in rat cardiac muscle at resting and extended sarcomere lengths. *J. Physiol.* 517:831–837.
- Hongo, K., E. White, J.Y. Le Guennec, and C.H. Orchard. 1996. Changes in [Ca²⁺]_i, [Na⁺]_i and Ca²⁺ current in isolated rat ventricular myocytes following an increase in cell length. *J. Physiol.* 491:609–619.
- Kentish, J.C., H.E. ter Keurs, L. Ricciardi, J.J. Bucx, and M.I. Noble. 1986. Comparison between the sarcomere length-force relations of intact and skinned trabeculae from rat right ventricle. Influence of calcium concentrations on these relations. *Circ. Res.* 58:755–768.
- Konhilas, J.P., T.C. Irving, and P.P. de Tombe. 2002. Myofilament calcium sensitivity in skinned rat cardiac trabeculae: role of inter-filament spacing. *Circ. Res.* 90:59–65.
- Le Guennec, J.Y., N. Peineau, J.A. Argibay, K.G. Mongo, and D. Garnier. 1990. A new method of attachment of isolated mammalian ventricular myocytes for tension recording: length dependence of passive and active tension. *J. Mol. Cell. Cardiol.* 22:1083–1093.
- Lillywhite, H.B., K.C. Zippel, and A.P. Farrell. 1999. Resting and maximal heart rates in ectothermic vertebrates. *Comp. Biochem. Physiol. A Mol. Integr. Physiol.* 124:369–382.
- Natali, A.J., L.A. Wilson, M. Peckham, D.L. Turner, S.M. Harrison, and E. White. 2002. Different regional effects of voluntary exercise on the mechanical and electrical properties of rat ventricular myocytes. *J. Physiol.* 541:863–875.
- Page, S. 1964. Filament lengths in resting and excited muscles. *Proc. R. Soc. Lond. B. Biol. Sci.* 160:460–466.
- Peters, G.W., D.A. Steiner, J.A. Rigoni, A.D. Mascilli, R.W. Schnepf, and S.P. Thomas. 2005. Cardiorespiratory adjustments of homing pigeons to steady wind tunnel flight. *J. Exp. Biol.* 208:3109–3120.
- Rantin, F.T., H. Gesser, A.L. Kalinin, C.D.R. Guerra, J.C. DeFreitas, and W.R. Driedzic. 1998. Heart performance; Ca²⁺ regulation and energy metabolism at high temperatures in *Bathygobius soporator*, a tropical marine teleost. *J. Therm. Biol.* 23:31–39.
- Robinson, T.F., and S. Winegrad. 1979. The measurement and dynamic implications of thin filament lengths in heart muscle. *J. Physiol.* 286:607–619.
- Shiels, H.A., M. Vornanen, and A.P. Farrell. 2000. Temperature-dependence of L-type Ca²⁺ channel current in atrial myocytes from rainbow trout. *J. Exp. Biol.* 203:2771–2780.
- ter Keurs, H.E., W.H. Rijnsburger, R. van Heuningen, and M.J. Nagelsmit. 1980. Tension development and sarcomere length in rat cardiac trabeculae. Evidence of length-dependent activation. *Circ. Res.* 46:703–714.
- Vornanen, M. 1998. L-type Ca²⁺ current in fish cardiac myocytes: effects of thermal acclimation and beta-adrenergic stimulation. *J. Exp. Biol.* 201:533–547.
- White, E., M.R. Boyett, and C.H. Orchard. 1995. The effects of mechanical loading and changes of length on single guinea-pig ventricular myocytes. *J. Physiol.* 482:93–107.
- White, E., J.Y. Le Guennec, J.M. Nigretto, F. Gannier, J.A. Argibay, and D. Garnier. 1993. The effects of increasing cell length on auxotonic contractions; membrane potential and intracellular calcium transients in single guinea-pig ventricular myocytes. *Exp. Physiol.* 78:65–78.
- Wu, Y., O. Cazorla, D. Labeit, and H. Granzier. 2000. Changes in titin and collagen underlie diastolic stiffness diversity of cardiac muscle. *J. Mol. Cell. Cardiol.* 32:2151–2162.